

Current fluctuations in the transient regime: An exact formulation for mesoscopic systems

Zimin Feng,¹ Joseph Maciejko,^{1,*} Jian Wang,² and Hong Guo¹

¹Centre for the Physics of Materials and Department of Physics, McGill University, Montreal, Quebec, Canada H3A 2T8

²Department of Physics, The University of Hong Kong, Hong Kong, China

(Received 21 September 2007; published 4 February 2008)

We report a theoretical analysis of current-current correlations in an arbitrary noninteracting mesoscopic phase-coherent device connected to arbitrary noninteracting external leads, in response to the sharp turning off of the bias voltage. Based on the Keldysh nonequilibrium Green's function formalism, we provide an exact analytical solution to the time-dependent current-current correlations in the far from equilibrium, nonlinear response regime. An important feature of our theory is that it does not rely on the commonly used wideband approximation so that the full electronic structure of the device leads is taken into account. As such, our theory provides a way to perform calculations of transient current fluctuations from first principles on realistic systems. We apply the exact formulation to a two-probe transport junction with the Lorentzian linewidth and investigate the time-dependent behavior of the current-current correlations when the voltage bias is abruptly turned off.

DOI: [10.1103/PhysRevB.77.075302](https://doi.org/10.1103/PhysRevB.77.075302)

PACS number(s): 73.63.-b, 72.10.Bg, 72.30.+q, 85.35.-p

I. INTRODUCTION

Electric current flowing inside a conductor can fluctuate with time due to the granularity of the charge carriers. Such fluctuation gives rise to the notion of shot noise that has been measured in various experimental setups.^{1,2} The spectra of current fluctuations contain useful information about the charge carriers in the current, including electron kinetics,³ correlations of electronic wave functions,⁴ and quasiparticle charge.^{5,6} In the experiment of Ref. 5 on the fractional quantum Hall effect, both the power of shot noise $S=2Q\bar{I}_e$ and the average charge current \bar{I}_e were measured simultaneously, and the ratio gave $Q=e/3$ which is the expected quasiparticle charge of the $\nu=1/3$ fractional quantum Hall state, with e the bare electron charge. Similarly, the measurements reported in Ref. 6 of current-current correlations in a normal-superconductor tunnel junction produced $Q=2e$, the charge of a Cooper pair. The information gained by these measurements, for example, the quasiparticle charge, is not contained in the average current alone.¹ For a normal system, it is also known that the current correlation between different measuring probes (cross-correlation) is negative for fermions and positive for bosons.^{7,8,11}

A classical conductor is characterized by the Poissonian noise,⁹ where the current fluctuation $\langle(\Delta I)^2\rangle$ in a frequency range $\Delta\nu$ is proportional to the electrical current I : $\langle(\Delta I)^2\rangle=2QI\Delta\nu$, where Q is the carrier charge. For a quantum conductor, the fluctuations are also influenced by two other physical factors: the Pauli exclusion principle and the Coulomb interaction. The Pauli exclusion reduces the classical noise by a factor proportional to $(1-T)$ for each transmission channel, assuming the transmission coefficient T to be insensitive to carrier energy.^{10,11} The Coulomb interaction, on the other hand, can contribute to reduce or enhance shot noise depending on system details. Shot noise can be characterized by the Fano factor $\mu\equiv S/(2e\bar{I}_e)$, which equals unity for classical conductors with completely uncorrelated transport of particles.

While most of the literature on current fluctuations and noise in the quantum regime has focused on linear steady-state transport, the fluctuations in the *transient* current are also of great interest. An example of transient noise measurement has been reported in Ref. 12 where noise at driving frequencies up to 250 GHz has been detected in a two-dimensional electron gas nanostructure. Indeed, a very serious challenge in mesoscopic device physics has been the understanding of *transient transport dynamics*. This includes such issues as understanding how fast or how slow a quantum device can turn on and/or off a current. The importance of transient phenomena is also highlighted by many high frequency transport measurements, such as photon-assisted tunneling,¹³ electron turnstiles,¹⁴ real-time electron dynamics,¹⁵ high frequency noise spectra,¹² quantum RLC circuits,¹⁶⁻¹⁸ parametric pumping,^{19,20} and ultrasensitive electrometers.²¹

The purpose of this paper is to report a theoretical investigation of the current-current correlations in the transient quantum transport regime. In particular, we calculate current correlations when the bias voltage of a two-probe quantum device is abruptly turned off. Namely, we consider a situation in which at times $t<0$, the device is in a steady state under bias Δ , and at time $t=0$, this bias is suddenly turned off to zero. Under such a step-shaped bias, the transport current I goes from a finite steady-state value I_0 for $t<0$ to zero for $t\geq 0$. When the electronic structures of the leads and of the device scattering region are taken into account, it is a very difficult problem to calculate the time-dependent current-current correlation. However, for a sharp step-down bias pulse, we discover that the time-dependent problem can be solved *exactly* for noninteracting systems. We report this solution in the rest of the paper.

Our theory for the current-current correlation builds upon a recently developed formalism for solving the time-dependent current $I(t)$ in mesoscopic phase-coherent devices driven by sharp step-shaped voltage pulses.²² The formalism is based on the Keldysh nonequilibrium Green's functions (NEGFs) and it provides an *exact* analytical solution to the

transport equations in the far from equilibrium, nonlinear response and noninteracting regime. The essential feature of the formalism²² is that it does not rely on the commonly used wideband limit (WBL). The WBL assumes that the coupling between device scattering region and electrodes is independent of energy so that any electronic structure of the electrodes is ignored. This is used for analytical work where the WBL drastically simplifies mathematical derivations, but it is a crude approximation for many practical situations and indeed, in nanoscale systems, electrode materials are characterized by complicated band structures which lead to non-trivial features in the density of states such as peaks, dips, gaps, and the van Hove singularities.²³ Since the formalism of Ref. 22 provides a way to perform transient transport calculations beyond the WBL, it is the starting point of the present work.

In the next section, we present a detailed derivation of the current-current correlation using NEGF. Since we can solve the problem exactly, it should be useful to present the theory in more detail to interested readers. In Sec. III, we apply our theory to a two-probe transport junction where the device scattering region is a single-level quantum well, and the electrodes are characterized by a finite band Lorentzian line shape. Finally, a short summary is presented in Sec. IV. Appendix can be found at the end where some derivation details are presented for interested readers.

II. THEORY

To calculate the current-current fluctuations in the transient regime after the bias voltage is abruptly turned off, we make use of the Keldysh nonequilibrium Green's function formalism.²⁴ We consider a two-probe nanostructure described by the following Hamiltonian:

$$H = \sum_{\mathbf{k}\alpha} \epsilon_{\mathbf{k}\alpha}(t) c_{\mathbf{k}\alpha}^\dagger c_{\mathbf{k}\alpha} + \sum_{mn} \epsilon_{mn}(t) d_m^\dagger d_n + \sum_{\mathbf{k}\alpha, n} (t_{\mathbf{k}\alpha n} c_{\mathbf{k}\alpha}^\dagger d_n + t_{\mathbf{k}\alpha n}^* d_n^\dagger c_{\mathbf{k}\alpha}), \quad (1)$$

where $\alpha=L,R$ indicates the left and right leads. Here, $\epsilon_{\mathbf{k}\alpha}(t)$ is the energy of state \mathbf{k} in lead α and $c_{\mathbf{k}\alpha}$ is the annihilation operator for electrons there. Similarly, $\epsilon_{mn}(t)$ is the Hamiltonian of the device scattering region in a given single-particle basis $\{|n\rangle\}$ with d_n as the corresponding annihilation operator. The first two terms in Eq. (1) describe the isolated (unconnected) leads and scattering region, respectively. The last term describes hopping processes between the leads and the scattering region with the coupling matrix $t_{\mathbf{k}\alpha n}$.

In our calculations, we assume that the single-particle energies follow adiabatically the time dependence of the external fields.²⁴⁻²⁶ As pointed out in Ref. 25, this assumption assigns an upper limit ω_c of roughly tens of terahertz to the spectral content of the time-dependent perturbation. In this work, we will consider external bias with a step function time dependence (step-down bias), which corresponds roughly to a pulse rise time $\tau \sim \pi/\omega_c$ which is on the order of tens of femtoseconds. Since electron dynamics are usually in the picosecond range, we can safely model the bias turning off by a perfectly sharp down step. Hence, the bias applied to the left lead $\Delta_L(t)$ is given as

$$\Delta_L(t) = \Delta\theta(-t), \quad (2)$$

where Δ on the right-hand side is a constant and $\theta(t)$ is the Heaviside function, $\theta(t<0)=0$ and $\theta(t>0)=1$. Within the adiabatic approximation, the energy levels of the left lead become $\epsilon_{\mathbf{k}L}(t) = \epsilon_{\mathbf{k}L}(0) + \Delta_L(t)$.

The electric current operator is readily obtained by the equation of motion,²⁴ $\hat{I}_\alpha(t) \equiv -e d\hat{N}_\alpha/dt$, where e is the elementary charge and $\hat{N}_\alpha = \sum_{\mathbf{k}\alpha} c_{\mathbf{k}\alpha}^\dagger c_{\mathbf{k}\alpha}$ is the number operator for lead α . Applying the equation of motion, one obtains²⁴

$$\hat{I}_\alpha(t) = -i \sum_{\mathbf{k}n} t_{\mathbf{k}\alpha n} c_{\mathbf{k}\alpha}^\dagger(t) d_n(t) + \text{H.c.}, \quad (3)$$

where we have fixed units such that $e = \hbar = 1$. From this operator form, one obtains the time-dependent current $I_\alpha(t)$ by taking expectation values.

The current-current fluctuations defined as $F_\alpha(t) \equiv \langle \Delta I_\alpha(t)^2 \rangle = \langle I_\alpha^2(t) \rangle - \langle I_\alpha(t) \rangle^2$ can be calculated using Eq. (3). We obtain

$$F_L(t) = - \sum_{\mathbf{k}\mathbf{k}'mn} (t_{\mathbf{k}Lm} t_{\mathbf{k}'Ln} \langle \langle c_{\mathbf{k}L}^\dagger d_m c_{\mathbf{k}'L}^\dagger d_n \rangle \rangle - \text{o.o.}) + t_{\mathbf{k}Lm}^* t_{\mathbf{k}'Ln}^* \langle \langle d_m^\dagger c_{\mathbf{k}L} d_n^\dagger c_{\mathbf{k}'L} \rangle \rangle - \text{o.o.}) - t_{\mathbf{k}Lm} t_{\mathbf{k}'Ln}^* \langle \langle c_{\mathbf{k}L}^\dagger d_m d_n^\dagger c_{\mathbf{k}'L} \rangle \rangle - \text{o.o.}) - t_{\mathbf{k}Lm}^* t_{\mathbf{k}'Ln} \langle \langle d_m^\dagger c_{\mathbf{k}L} c_{\mathbf{k}'L}^\dagger d_n \rangle \rangle - \text{o.o.}), \quad (4)$$

where the notation o.o. stands for a two-by-two pairing of the operators without changing their orders. For example, if \hat{a} , \hat{b} , \hat{c} , and \hat{d} are operators, then $[\langle \hat{a}\hat{b}\hat{c}\hat{d} \rangle - \text{o.o.}]$ stands for $[\langle \hat{a}\hat{b}\hat{c}\hat{d} \rangle - \langle \hat{a}\hat{b} \rangle \langle \hat{c}\hat{d} \rangle]$.

Applying Wick's theorem,²⁷ it is not difficult to show that all the o.o. pairings cancel and Eq. (4) becomes

$$F_L(t) = - \sum_{\mathbf{k}\mathbf{k}'mn} (t_{\mathbf{k}Lm} t_{\mathbf{k}'Ln} \langle c_{\mathbf{k}L}^\dagger d_n \rangle \langle d_m c_{\mathbf{k}'L}^\dagger \rangle + t_{\mathbf{k}Lm}^* t_{\mathbf{k}'Ln}^* \langle d_m^\dagger c_{\mathbf{k}'L} \rangle \langle c_{\mathbf{k}L} d_n^\dagger \rangle - t_{\mathbf{k}Lm} t_{\mathbf{k}'Ln}^* \langle c_{\mathbf{k}L} d_n^\dagger \rangle \langle c_{\mathbf{k}'L}^\dagger d_m \rangle - t_{\mathbf{k}Lm}^* t_{\mathbf{k}'Ln} \langle d_m^\dagger c_{\mathbf{k}'L} \rangle \langle c_{\mathbf{k}L}^\dagger d_n \rangle) \times \langle c_{\mathbf{k}'L}^\dagger c_{\mathbf{k}L} \rangle,$$

which, in turn, can be written in terms of the nonequilibrium Green's functions,

$$F_L(t) = - \sum_{\mathbf{k}\mathbf{k}'mn} (t_{\mathbf{k}Lm} t_{\mathbf{k}'Ln} G_{n,\mathbf{k}L}^<(t,t) G_{m,\mathbf{k}'L}^>(t,t) + t_{\mathbf{k}Lm}^* t_{\mathbf{k}'Ln}^* G_{\mathbf{k}'mL,m}^<(t,t) G_{\mathbf{k}L,n}^>(t,t) - t_{\mathbf{k}Lm} t_{\mathbf{k}'Ln}^* G_{\mathbf{k}'L,\mathbf{k}L}^<(t,t) G_{mn}^>(t,t) - t_{\mathbf{k}Lm}^* t_{\mathbf{k}'Ln} G_{nm}^<(t,t) G_{\mathbf{k}L,\mathbf{k}'L}^>(t,t)),$$

where the time dependence is emphasized. The NEGFs that mixes operators in the leads and in the scattering region are defined as

$$G_{n,\mathbf{k}L}^<(t,t') \equiv i\langle c_{\mathbf{k}L}^\dagger(t')d_n(t) \rangle,$$

$$G_{m,\mathbf{k}'L}^>(t,t') \equiv -i\langle d_m(t)c_{\mathbf{k}'L}^\dagger(t') \rangle. \quad (5)$$

The NEGFs for the scattering region and for the leads, $G_{nm}^<$ and $G_{\mathbf{k}'L,\mathbf{k}L}^<$, are defined in similar manner,

$$G_{nm}^<(t,t') \equiv i\langle d_m^\dagger(t')d_n(t) \rangle,$$

$$G_{\mathbf{k}'L,\mathbf{k}L}^<(t,t') \equiv i\langle c_{\mathbf{k}L}^\dagger(t')c_{\mathbf{k}'L}(t) \rangle. \quad (6)$$

Following Ref. 25 and taking advantage of the Langreth analytical continuation theorem,²⁸ the mixed NEGF [Eq. (5)] can be expressed in terms of the NEGFs of the scattering region and the leads [Eq. (6)],

$$G_{n,\mathbf{k}L}^<,>(t,t') = \sum_m \int dt_1 (G_{nm}^r(t,t_1)t_{\mathbf{k}Lm}^* g_{\mathbf{k}L}^<,>(t_1,t') + G_{nm}^<,>(t,t_1)t_{\mathbf{k}Lm}^* g_{\mathbf{k}L}^a(t_1,t')),$$

where the Green functions of the leads, $g_{\mathbf{k}L}^x(t,t')$, are defined as

$$g_{\mathbf{k}L}^r(t,t') = -i\theta(t-t')\langle \{c_{\mathbf{k}L}(t), c_{\mathbf{k}L}^\dagger(t')\} \rangle_0,$$

$$g_{\mathbf{k}L}^<(t,t') = i\langle c_{\mathbf{k}L}^\dagger(t')c_{\mathbf{k}L}(t) \rangle_0.$$

Here, the subscript “0” indicates that the average is taken with respect to the ground state of isolated leads; therefore, these Green functions are known. Similarly,

$$G_{\mathbf{k}L,n}^<,>(t,t') = \sum_m \int dt_1 (g_{\mathbf{k}L}^<,>(t,t_1)t_{\mathbf{k}Lm} G_{mn}^a(t_1,t') + g_{\mathbf{k}L}^r(t,t_1)t_{\mathbf{k}Lm} G_{mn}^<,>(t_1,t')),$$

and finally,

$$G_{\mathbf{k}L,\mathbf{k}'L}^<,>(t,t') = g_{\mathbf{k}L}^<,>(t,t')\delta_{\mathbf{k}L,\mathbf{k}'L} + \sum_n \int dt_1 (G_{\mathbf{k}L,n}^r(t,t_1)t_{\mathbf{k}'Ln}^* g_{\mathbf{k}'L}^<,>(t_1,t') + G_{\mathbf{k}L,n}^<,>(t,t_1)t_{\mathbf{k}'Ln}^* g_{\mathbf{k}'L}^a(t_1,t')),$$

where the mixed retarded Green's function is

$$G_{\mathbf{k}L,n}^r(t,t') = \sum_m \int dt_1 g_{\mathbf{k}L}^r(t,t_1)t_{\mathbf{k}Lm} G_{mn}^r(t_1,t'). \quad (7)$$

With the help of the following relations,

$$[G^r(t,t')]^\dagger = G^a(t',t),$$

$$[G^<,>(t,t')]^\dagger = -G^<,>(t',t),$$

the time-dependent fluctuation $F_L(t)$ can now be expressed in terms of the Green functions of the scattering region,

$$F_L(t) = \text{Tr} \left\{ -2 \text{Re} \left[\left(\int dt_1 G^r(t,t_1)\Sigma_L^<(t_1,t) + G^<(t,t_1)\Sigma_L^a(t_1,t) \right) \left(\int dt_1 G^r(t,t_1)\Sigma_L^>(t_1,t) + G^>(t,t_1)\Sigma_L^a(t_1,t) \right) \right] + G^>(t,t) \right. \\ \times \left[\int dt_1 \int dt_2 [2i \text{Im}(\Sigma_L^r(t,t_1)G^r(t_1,t_2)\Sigma_L^<(t_2,t)) + \Sigma_L^r(t,t_1)G^<(t_1,t_2)\Sigma_L^a(t_2,t)] + \Sigma^<(t,t) \right] + G^<(t,t) \\ \times \left. \left[\int dt_1 \int dt_2 [2i \text{Im}(\Sigma_L^r(t,t_1)G^r(t_1,t_2)\Sigma_L^>(t_2,t)) + \Sigma_L^r(t,t_1)G^>(t_1,t_2)\Sigma_L^a(t_2,t)] + \Sigma^>(t,t) \right] \right\}, \quad (8)$$

where the self-energies of the leads are defined as

$$\Sigma_{\alpha,mn}^x(t_1,t_2) \equiv \sum_{\mathbf{k}} t_{\mathbf{k}am}^* g_{\mathbf{k}\alpha}^x(t_1,t_2)t_{\mathbf{k}an},$$

with $x = \langle, \rangle, r, a$. In terms of the linewidth function $\Gamma_\alpha(\epsilon)$, the self-energies can be written as²²

$$\Sigma_\alpha^<(t,t') = i \int \frac{d\epsilon}{2\pi} \exp[-i\epsilon(t-t')] \\ \times \exp \left[-i \int_{t'}^t \Delta_\alpha(\tau) d\tau \right] F(\epsilon) \Gamma_\alpha(\epsilon), \quad (9)$$

and

$$\Sigma_\alpha^r(t,t') = -i\theta(t-t') \int \frac{d\omega}{2\pi} \exp[-i\omega(t-t')] \\ \times \exp \left[-i \int_{t'}^t \Delta_\alpha(\tau) d\tau \right] \Gamma_\alpha(\omega), \quad (10)$$

where $F(\epsilon)$ is the Fermi distribution function. In the rest of the work, we consider the zero-temperature limit and can always write Eq. (9) as

$$\Sigma_{\alpha}^{<}(t,t') = i \int_{-\infty}^{E_F} \frac{d\epsilon}{2\pi} \exp[-i\epsilon(t-t')] \times \exp \left[-i \int_{t'}^t \Delta_{\alpha}(\tau) d\tau \right] \Gamma_{\alpha}(\epsilon). \quad (11)$$

In practical calculations (see below), the greater Green's function $G^{>}(t,t')$ is expressed via the lesser, retarded, and advanced Green's functions. For the down-step pulse of Eq. (2), Maciejko *et al.*²² has derived these Green functions exactly in terms of the *steady-state* NEGF for the connected lead-device-lead (LDL) system. In particular, taking the time-independent pieces of the entire LDL Hamiltonian as the unperturbed part of a perturbation theory, and taking the time-dependent bias potential [Eq. (2)] as the perturbation, the Dyson equation for G^r can be written as²²

$$\begin{aligned} G^r(t,t') &= \tilde{G}^r(t-t') + \int dt_1 \tilde{G}^r(t-t_1) \Delta_c \theta(t_1) G^r(t_1,t') \\ &+ \int dt_1 \int dt_2 \tilde{G}^r(t-t_1) \\ &\times \sum_{\alpha} \left[\exp \left[-i \int_{t_2}^{t_1} dt' \Delta_{\alpha}(t') \right] - 1 \right] \tilde{\Sigma}_{\alpha}^r(t_1 \\ &- t_2) G^a(t_2,t'), \end{aligned} \quad (12)$$

where $\Delta_c(t)$ and $\Delta_{\alpha}(t)$ are external bias fields in the device scattering region and in the leads, respectively. In our case, $\Delta_L(t) = \Delta \theta(-t)$ is given by Eq. (2) and $\Delta_R(t)$ is set to zero. Here, $\Delta_c(t)$ is taken to be half of $\Delta_L(t)$ assuming a symmetrical device structure. In Eq. (12), the quantity $\tilde{G}^r(t-t')$ is a time-translationally invariant Green's function, i.e., the equilibrium Green's function for the unperturbed LDL Hamiltonian. For a given device Hamiltonian, its equilibrium Green's function $\tilde{G}^r(t-t')$ can be calculated in many ways and an example will be given below.

The above Dyson equation [Eq. (12)] for a downward-step pulse has been solved exactly in our previous paper [see Eqs. (13), (17), and (22) of Ref. 22]. Here, we quote these results and rewrite that solution as

$$\begin{aligned} \check{G}^r(t > 0, t' < 0) &= \tilde{G}^r(t-t') \\ &+ \int \frac{d\omega d\omega'}{2\pi 2\pi i} \tilde{G}^r(\omega) \tilde{G}^r(\omega') e^{-i\omega t + i\omega' t'} \\ &\times \left[\frac{\Delta_c}{\omega - \omega' - i0^+} \right. \\ &\left. + \frac{\Delta(\tilde{\Sigma}_L^r(\omega' - \Delta) - \tilde{\Sigma}_L^r(\omega))}{(\omega' - \omega - \Delta + i0^+)(\omega' - \omega + i0^+)} \right], \end{aligned} \quad (13)$$

and the total Green's function is

$$G(t,t') = \begin{cases} \bar{G}(t-t') & \text{if } t < 0 \text{ and } t' < 0 \\ \check{G}(t,t') & \text{if } t > 0 \text{ and } t' < 0 \\ \tilde{G}(t-t') & \text{if } t > 0 \text{ and } t' > 0 \\ 0 & \text{otherwise,} \end{cases} \quad (14)$$

where 0^+ is a positive infinitesimal number, $\bar{G}^r(\omega)$ is the Fourier transform of steady-state retarded Green's function $\bar{G}^r(t-t')$, and $\tilde{G}^r(\omega)$ is the Fourier transform of the *equilibrium* retarded Green's function $\tilde{G}^r(t-t')$. In the following, all tilded functions refer to equilibrium situation (zero bias) and all barred functions refer to steady state situations (finite bias). By setting $t=0$, one can readily check that the above solution satisfies $G^r(0,t') = \bar{G}^r(0-t')$, and by setting $t'=0$, that $G^r(t,0) = \tilde{G}^r(t-0)$. These are the correct limits since for times $t < 0$, the system is in a nonequilibrium steady state under bias Δ , while after $t=0$, the system is in equilibrium without any bias voltage.

To go further and for lack of space, we refer interested readers to Ref. 22 for explicit expressions of the NEGFs, $\bar{G}^r(t-t')$ and $G^{<}(t,t')$. Here, we point out that all the Green functions are calculated^{22,24} via a Green-function-like quantity defined as

$$A_{\alpha}(\epsilon,t) \equiv \int_{-\infty}^t dt' \exp[i\epsilon(t-t')] \exp \left[-i \int_t^{t'} d\tau \Delta(\tau) \right] G^r(t,t').$$

The use of the function $A_{\alpha}(\epsilon,t)$ simplifies the derivations and its explicit expressions for a downward-step pulse are

$$A_{\alpha}(\epsilon,t < 0) = \bar{G}^r(\epsilon + \Delta_{\alpha}),$$

$$\begin{aligned} A_{\alpha}(\epsilon,t > 0) &= \tilde{G}^r(\epsilon) + \int \frac{d\omega}{2\pi} \frac{e^{-i(\omega-\epsilon)t} \tilde{G}^r(\omega)}{\omega - \epsilon - \Delta_{\alpha} - i0^+} \\ &\times \left[\frac{\Delta_{\alpha}}{\omega - \epsilon - i0^+} + \left(\Delta_c - \sum_{\beta} \Delta_{\beta} Y_{\alpha\beta}(\omega, \epsilon) \right) \right. \\ &\left. \times \bar{G}^r(\epsilon + \Delta_{\alpha}) \right], \end{aligned} \quad (15)$$

with

$$Y_{\alpha\beta}(\omega, \epsilon) \equiv \frac{\tilde{\Sigma}_{\beta}^r(\omega) - \tilde{\Sigma}_{\beta}^r(\epsilon + \Delta_{\alpha} - \Delta_{\beta})}{\omega - \epsilon - \Delta_{\alpha} + \Delta_{\beta} \pm i0^+}, \quad (16)$$

where the sign of the infinitesimal imaginary part $i0^+$ can be arbitrarily chosen or the $i0^+$ discarded altogether.²²

Finally, we rewrite the analytical expression [Eq. (8)] for the current fluctuations in the following form, which will be used for numerical computation in the next section of the paper:

$$\begin{aligned}
F_L(t) = \text{Tr} \left\{ -2 \text{Re} \left(\int dt_1 G^r(t, t_1) \Sigma_L^<(t_1, t) + G^<(t, t_1) \Sigma_L^a(t_1, t) \right)^2 + G^>(t, t) \left[\int dt_1 \int dt_2 [2i \text{Im}(\Sigma_L^r(t, t_1) G^r(t_1, t_2) \Sigma_L^<(t_2, t)) \right. \right. \\
+ \Sigma_L^r(t, t_1) G^<(t_1, t_2) \Sigma_L^a(t_2, t)] + \Sigma^<(t, t) \left. \right] + G^<(t, t) \left[\int dt_1 \int dt_2 [2i \text{Im}(\Sigma_L^r(t, t_1) G^r(t_1, t_2) \Sigma_L^<(t_2, t)) \right. \\
\left. \left. - \Sigma_L^r(t, t_1) G^r(t_1, t_2) \Sigma_L^a(t_2, t) + \Sigma_L^r(t, t_1) G^<(t_1, t_2) \Sigma_L^a(t_2, t) + 2i \text{Im}(\Sigma_L^r(t, t_1) G^r(t_1, t_2) \Sigma_L^a(t_2, t))] + \Sigma^>(t, t) \right] \right\}, \quad (17)
\end{aligned}$$

where all the greater Green's functions are substituted with the equivalent expression,

$$G^>(t_1, t_2) = G^<(t_1, t_2) + G^r(t_1, t_2) - G^a(t_1, t_2). \quad (18)$$

One can check that Eq. (17) is exactly equivalent to Eq. (8). Equation (17) is the main result of this work. With this preliminary work, we can calculate Eq. (17) at zero-temperature term by term. These are tedious calculations and we present a detailed derivation of the first term in Appendix. The final expressions for other terms are also listed there.

III. NUMERICAL RESULTS

In the following, we apply the exact analytical expression [Eq. (17)] to a two-probe system where the scattering region has a single energy level ϵ_0 . The electronic structure of the device leads is assumed to have a Lorentzian line shape,²⁹

$$\Gamma_\alpha(\epsilon) = \frac{\Gamma_\alpha W^2}{\epsilon^2 + W^2}, \quad (19)$$

where W is the bandwidth and Γ_α the linewidth amplitude of lead α . The equilibrium and steady-state Green's functions for this model have been solved exactly in Ref. 22 and are substituted into Eq. (17) to calculate the current fluctuations driven by the step-down pulse. In the following numerical evaluation of Eq. (17), the energy level ϵ_0 is set to zero. The time is measured in units of \hbar/Γ , where $\Gamma = \sum_\alpha \Gamma_\alpha$, the current in units of $e\Gamma/\hbar$, and the energy in units of Γ . Also, all results shown here are for the *left* lead, and we shall henceforth omit the L subscript. Experimentally, Fujisawa *et al.*³⁰ achieved $\Gamma \sim 1-5 \mu\text{eV}$. Gabelli *et al.*¹⁷ further showed that Γ can be experimentally controlled by a gate potential. Therefore, assuming $\Gamma \sim 1 \mu\text{eV}$ in a real experimental device, the time scale in our results corresponds to a frequency of $\sim 1.5 \text{ GHz}$ which is achievable experimentally.

In Fig. 1, we plot the current fluctuations $F(t)$ versus time t for several values of the bandwidth W when the Fermi level of the leads E_F aligns with the resonant level ϵ_0 . This is the on-resonance situation. The external bias is chosen to be 10Γ . For times $t < 0$, the system is in a steady state biased by a voltage Δ , and the fluctuation is a time-independent constant. When the bias is abruptly turned off at $t=0$, $F(t)$ decreases abruptly to its minimum and then gradually goes back to another constant for $t \gg 0$ which corresponds to fluctuations at equilibrium. As one expects, we find that a larger bandwidth W gives rise to larger steady-state fluctuations

$F(t < 0)$ (see main figure in Fig. 1). This is understandable because a larger bandwidth corresponds to a higher number of Bloch electrons incoming from the leads and traversing the scattering region. The depth of the dip in $F(t)$ immediately after $t=0$ is found to be roughly proportional to W and rather insensitive to Δ (see Fig. 2 below). The inset of Fig. 1 shows the time-dependent current $I(t)$ for different values of W . The current decays from a finite initial value I_0 to zero at large times. For small bandwidths W , the instantaneous current $I(t)$ can *increase* following the step-down pulse at $t=0$. This peculiar behavior is truly a finite-bandwidth effect as discussed before.^{22,31}

In Fig. 2, we plot the current fluctuations $F(t)$ versus time t for several different bias step heights Δ with bandwidth $W=5\Gamma$. Once again, for $t < 0$ and $t \gg 0$, fluctuations take constant values corresponding to those in steady state and at equilibrium, respectively. For a nonequilibrium steady state, the bias dependence of *shot noise* has been discussed in Ref. 32 where it has been shown that a finite bias can suppress shot noise in steady state. Although $F(t)$ is not directly shot noise, its behavior in Fig. 2 shows a similar suppression for $t < 0$ compared with that for $t \gg 0$. The inset of Fig. 2 displays the time-dependent current $I(t)$ for several values of Δ .

Off-resonance time-dependent current fluctuations ($E_F \neq \epsilon_0$) also display interesting features. In Fig. 3, we plot $F(t)$

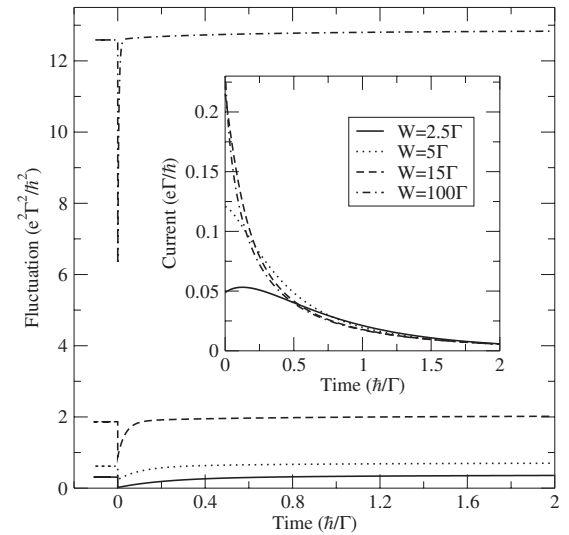


FIG. 1. On-resonance current fluctuations $F(t)$ versus time t for several values of the bandwidth W . The inset shows the corresponding current $I(t)$ versus t . The bias Δ is set to 10Γ .

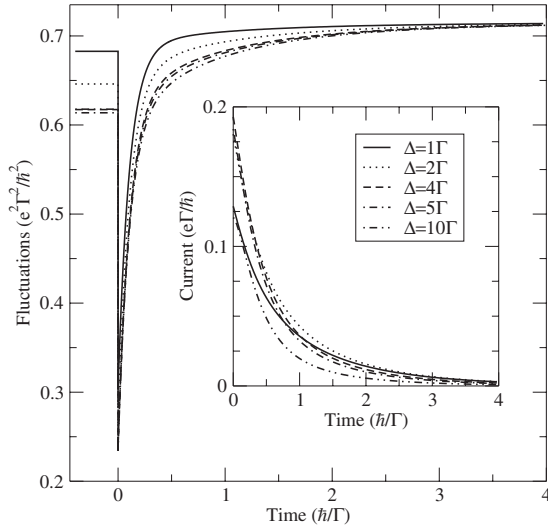


FIG. 2. On-resonance current fluctuations $F(t)$ versus time t for several values of the bias Δ . The inset shows the corresponding current $I(t)$ versus t . The bandwidth W is set to 5Γ .

versus t for several values of W when $E_F - \epsilon_0 = -2\Gamma$, for the same bias $\Delta = 10\Gamma$. The time-dependent current $I(t)$ is plotted in the inset where it can dip to negative values after the voltage is turned off but eventually approaches zero for $t \gg 0$. Such a negative current following a voltage pulse has also been found before.^{22,31} The fluctuation $F(t)$ has more features than for the on-resonance case. This is more clearly shown in Fig. 4 for different values of Δ . In particular, $F(t)$ dips to small values immediately after $t=0$, and then it rises to a maximum value before decaying to the equilibrium limit. The inset of Fig. 4 shows the corresponding behavior of the current $I(t)$. Finally, we comment that the sharp dips immediately after time $t=0$ in Figs. 1–3 come from the fact that the bias voltage is sharply turned off at $t=0$ in a step-

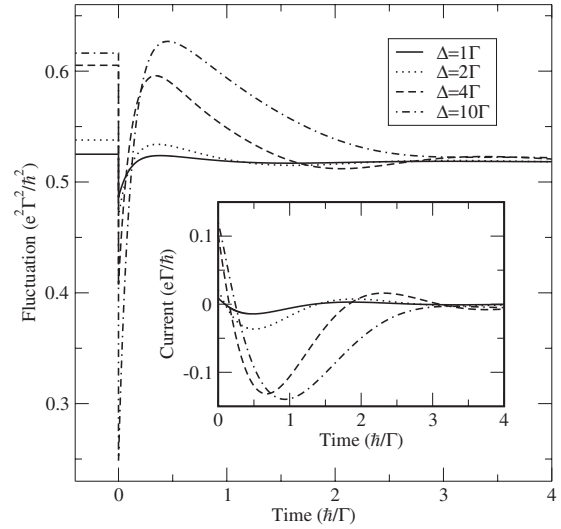


FIG. 4. Off-resonance current fluctuations $F(t)$ versus time t for several values of the bias Δ . The inset shows the corresponding current $I(t)$ versus t . The bandwidth W is set to 5Γ .

function-like manner, i.e., Eq. (2). As explained in Sec. II, such a sharp steplike turning off assigns an upper frequency limit of tens of terahertz. The main features of our results, including the dips of the correlators, are in the gigahertz range using realistic experimental parameters as discussed above. Therefore, these dips are real features of the electron dynamics for the sharp bias turning off.

To observe the time dependence of $F(t)$ more clearly, we subtract the equilibrium fluctuations and define $\delta F(t) \equiv -[F(t) - F(\infty)]$. In Fig. 5, we plot $\delta F(t)$ on a logarithmic scale versus t for the on-resonance parameters of Fig. 1. This plot shows that the time dependence of $F(t)$ under a down-step pulse is not a simple exponential. A closer examination of the analytical expressions for $F(t)$ (see Appendix) reveals

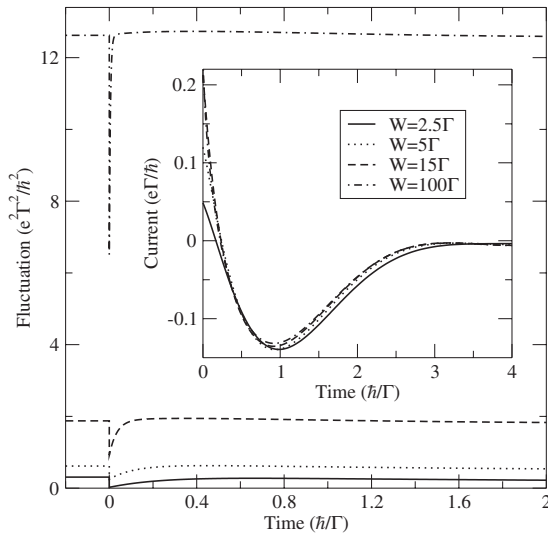


FIG. 3. Off-resonance current fluctuations $F(t)$ versus time t for several values of the bandwidth W . The inset shows the corresponding current $I(t)$ versus t . The bias Δ is set to 10Γ .

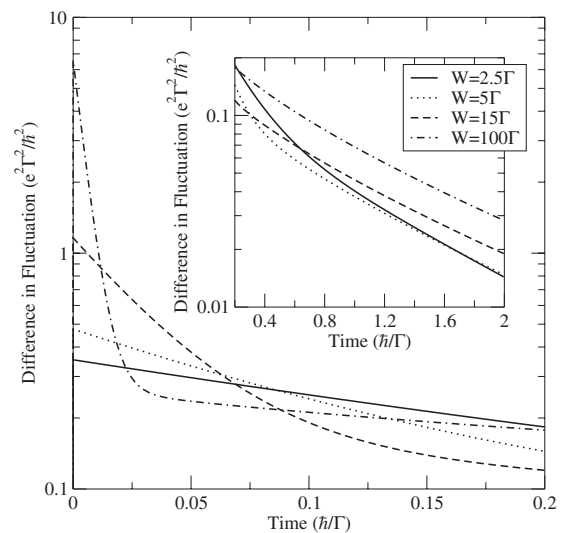


FIG. 5. Logarithmic-scale plot of $\delta F(t) \equiv -[F(t) - F(\infty)]$ for short times after turn off. The inset shows the behavior at larger times. The bias Δ is set to 10Γ .

that the decay time is related to the parameters Γ and W but not in a simple form. Generally, a wider bandwidth W gives a narrower peak in $\log \delta F(t)$ near $t=0$, which implies a shorter relaxation time. This result is consistent with the turnoff time of the current $I(t)$ itself.²² From the inset of Fig. 1, it is clear that the turnoff time is reduced with increasing W .

Since our calculation is carried out at zero temperature, the only source of fluctuation must be the quantum shot noise coming from the quasiparticle dynamics in the transport current $I(t)$. When there is no time-dependent field, in our problem, the quasiparticles are simply noninteracting electrons. As discussed in Introduction, quasiparticles with charges $e/3$ and $2e$ have been measured in the $\nu=1/3$ fractional quantum Hall state⁵ and in superconducting tunnel junctions,⁶ respectively. In the present problem, electrons are pushed to move forward by a bias voltage that is suddenly turned off at $t=0$. Such a time-dependent external field causes electrons to move in complicated time-dependent manner. If we consider the electrons as being “dressed” by a time-dependent potential, we may be able to analyze our fully quantum-mechanical result for current fluctuations in terms of an ideal *classical* Poissonian random process of quasiparticles flowing under the step-down voltage. In the following, we attempt such an interesting analysis.

For a homogeneous classical Poissonian random process X , we can write its average as³³

$$\langle X \rangle = \lambda \int d(\tau), \quad (20)$$

and its fluctuation as

$$\langle \sigma_X^2 \rangle = \lambda \int d\tau h^2(\tau), \quad (21)$$

where τ is the time parameter. Here, we may consider $h(\tau)$ to be the particle current contributed by one event, i.e., one particle going through the device. For our time-dependent problem, it is convenient to consider the probability parameter λ in the above equation as a function of time $\lambda=\lambda(t)$, such that $\langle X \rangle$ and $\langle \sigma_X^2 \rangle$ both become functions of t .

Next, we model the event $h(t)$ with a square function of constant height h and width τ_e . Namely, in the classical Poissonian process, there are many square-shaped “particles” randomly traversing the device. Later, we will see that we do not need τ_e for any practical purposes, but we do need to specify the parameter h . Having fixed the particle current with the parameter h this way, we attach to each particle an effective charge $x(t)$ (in units of the bare charge e) so as to obtain a charge current. Therefore, we replace $h(\tau)$ in Eqs. (20) and (21) with $x(t)h(\tau)$. Again, $x(t)$ represents the effective charge of the quasiparticles in the time-dependent current at time t , and we wish to fit this classical Poissonian process to the full quantum results presented in Figs. 1 and 2 to determine $x(t)$. The output of this analysis can be thought of as a time-dependent version of the Fano factor.³⁴

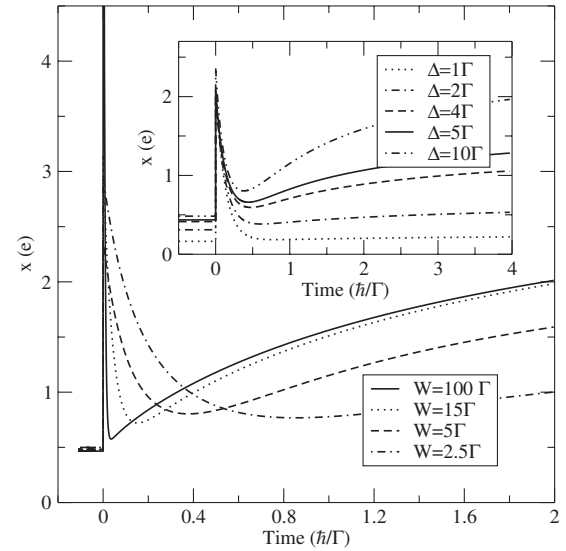


FIG. 6. Effective carrier charge $x(t)$ versus t at several bandwidths W for $\Delta=10\Gamma$. The sharp peak at $t=0$ is cut off for clarity. In particular, $x(0)$ reaches a value of 11 for $W=100\Gamma$. The inset shows $x(t)$ for several biases Δ with $W=5\Gamma$.

The parameter h is determined by fitting our quantum result for the steady state ($t<0$). In particular, we replace $x(t)$ with the Fano factor μ , and from Eqs. (20) and (21), we obtain

$$\frac{\sigma^2}{\langle I \rangle} = \mu h. \quad (22)$$

The Fano factor μ can be interpreted as the *effective* charge and it has been calculated in steady state³² from the transmission coefficient.³⁵ Here, $\langle I \rangle$ is the average steady-state current obtained from our quantum analysis above, i.e., the values of the current at $t=0^-$ in the insets of Figs. 1 and 2. The quantity σ^2 is just $\delta F(t) \equiv -[F(t) - F(\infty)]$ defined above for $t<0$ (in Fig. 5, we plot δF at $t \geq 0$). Fitting these expressions yields the parameter h .

Next, for finite times $t>0$, Eq. (22) is changed to

$$\frac{\sigma^2(t)}{\langle I(t) \rangle} = x(t)h. \quad (23)$$

We therefore obtain $x(t)$ as

$$x(t) = \frac{\sigma^2(t)}{h\langle I(t) \rangle}, \quad (24)$$

where $x(t)$ describes the effective charge of dressed particles in the time-dependent current considered as a classical Poissonian random process. Namely, if the classical particles have charge $x(t)$, then the classical fluctuations equal to the corresponding quantum result.

In Fig. 6, we plot the effective charge $x(t)$ versus t for different values of the bandwidth W . The inset shows $x(t)$ as a function of t for different values of the bias Δ . The parameters are chosen to be the same as in Fig. 1. For $t<0$, the effective charge $x(t)$ is just the steady-state Fano factor³² as

described above. At $t=0$, $x(t)$ has a sudden jump, well correlated with the current fluctuations $F(t)$ (see Fig. 1). This drastic increase of $x(t)$ can be understood as follows: classically, the charged particles “bunch up” at the moment when the bias is turned off. For $t \gg 0$, i.e., when t is of several tens of \hbar/Γ , we have checked that $x(t)$ approaches zero which is the equilibrium Fano factor for resonant transmission³⁵ (not shown in Fig. 6). For finite times t , $x(t)$ has a rather smooth but nonmonotonic time dependence.

IV. SUMMARY

We have derived an exact formula for analyzing current fluctuations in the transient regime for two-probe systems when the time-dependent current itself is driven by a bias voltage that is suddenly turned off. Our theory is valid for arbitrary noninteracting mesoscopic phase-coherent devices connected to arbitrary noninteracting external leads, in the far from equilibrium, nonlinear response regime. Our main result, Eq. (17), is the analytical solution of the time-dependent current fluctuations in the transient regime. Importantly, our theory does not rely on the commonly used wide-band approximation which neglects the electronic structure of the leads. As such, the exact formula [Eq. (17)] can be applied to realistic systems where the electronic structure of both leads and scattering region needs to be taken into account. This is especially useful as first principles methods for calculating equilibrium, and steady-state Green’s functions are now available^{36,37} for two-probe nanoelectronic devices. Therefore, our theory presented in this work can be applied, in principle, to analyze transient current-current correlations of realistic device structures including microscopic details of the system.

An application of the exact result [Eq. (17)] to a two-probe transport junction, where the leads have a Lorentzian linewidth shape, reveals interesting time dependence in the current fluctuations. Most notable is that when the bias voltage is abruptly turned off, the fluctuations do not follow a simple monotonic relaxation from their steady-state value at times $t < 0$ to their equilibrium value at $t \gg 0$. Rather, the fluctuations follow more complicated dynamics characterized by a very sharp dip immediately after $t=0$ before the eventual relaxation toward $t \gg 0$. The detailed relaxation dynamics are also dependent on various factors such as whether or not transport is on resonance, the bandwidth W in the leads, and the initial bias Δ . For the on-resonance case, we found that it is possible to interpret the transient quantum current fluctuations in terms of a classical random Poissonian process if the effective carrier charge in the classical current is a function of time.

ACKNOWLEDGMENTS

We gratefully acknowledge financial support of a RGC grant (HKU 7048/06P) from HKSAR (J.W), NSERC of Canada, FQRNT of Québec, and CIFAR (H.G.).

APPENDIX

In this Appendix, we present a detailed derivation of the final expression of the first term in Eq. (17). Other terms can

be obtained in the same manner. The first term of Eq. (17) is the following integral:

$$\int_{-\infty}^{\infty} dt_1 G^r(t, t_1) \Sigma_L^<(t_1, t) + G^<(t, t_1) \Sigma_L^a(t_1, t). \quad (\text{A1})$$

We are interested in times $t > 0$ after the bias is turned off. Using Eq. (11) for $\Sigma^<$, the first integral in expression (A1) becomes

$$\begin{aligned} & \int_{-\infty}^{\infty} dt_1 G^r(t, t_1) \Sigma_L^<(t_1, t) \\ &= \int_{-\infty}^0 dt_1 \check{G}(t, t_1) \int_{-\infty}^{E_F} \frac{d\epsilon}{2\pi} i e^{-\epsilon(t_1-t)} e^{-i\Delta t} \Gamma_L(\epsilon) \\ &+ \int_0^{\infty} dt_1 \tilde{G}(t-t_1) \int_{-\infty}^{E_F} \frac{d\epsilon}{2\pi} i e^{-\epsilon(t_1-t)} \Gamma_L(\epsilon), \end{aligned} \quad (\text{A2})$$

where $\check{G}^r(t, t_1)$ is the Green function for $t > 0$ and $t_1 < 0$, as defined in Eq. (13). It is a part of the total Green’s function [Eq. (14)]. Since the equilibrium Green’s function $\tilde{G}^r(t-t')$ and steady-state Green’s function $\bar{G}^r(t-t')$ have time-translational invariance, they can be Fourier transformed,

$$\tilde{G}(t-t') = \int \frac{d\omega}{2\pi} e^{-i\omega(t-t')} \tilde{G}(\omega). \quad (\text{A3})$$

The first term on the right-hand side of Eq. (A2) becomes

$$\begin{aligned} & \int_{-\infty}^0 dt_1 \check{G}(t, t_1) \int_{-\infty}^{E_F} \frac{d\epsilon}{2\pi} i e^{-\epsilon(t_1-t)} e^{-i\Delta t} \Gamma_L(\epsilon) \\ &= \int_{-\infty}^0 dt_1 \int_{-\infty}^{E_F} \frac{d\epsilon}{2\pi} \int \frac{d\omega}{2\pi} i \tilde{G}^r(\omega) \Gamma_L(\epsilon) e^{-i(\omega-\epsilon)t} e^{i(\omega-\epsilon-\Delta)t_1} \\ &+ \int_{-\infty}^0 dt_1 \int \frac{d\omega}{2\pi} \frac{d\omega_1}{2\pi i} \int_{-\infty}^0 \frac{d\epsilon}{2\pi} i \tilde{G}^r(\omega) \bar{G}^r(\omega_1) \Gamma_L(\epsilon) \\ &\times e^{i(\omega_1-\epsilon-\Delta)t_1} e^{-i(\omega-\epsilon)t} \\ &\times \left(\frac{\Delta_c}{\omega - \omega_1 - i0^+} + \frac{\Delta(\tilde{\Sigma}_L^r(\omega_1 - \Delta) - \tilde{\Sigma}_L^r(\omega))}{(\omega_1 - \omega - \Delta + i0^+)(\omega_1 - \omega + i0^+)} \right). \end{aligned} \quad (\text{A4})$$

The t_1 integration on the right-hand side can be carried out to give

$$\frac{1}{i(\omega - \epsilon - \Delta - i0^+)}$$

and

$$\frac{1}{i(\omega_1 - \epsilon - \Delta - i0^+)},$$

for the two terms of Eq. (A4), respectively. Therefore, the first term of Eq. (A4) becomes

$$\int \frac{d\omega}{2\pi} \int_{-\infty}^{E_F} \frac{d\epsilon}{2\pi} i\tilde{G}^r(\omega)\Gamma_L(\epsilon) \frac{e^{-i(\omega-\epsilon)t}}{\omega-\epsilon-\Delta-i0^+}, \quad (\text{A5})$$

which cannot be simplified further if the Green function $\tilde{G}^r(\omega)$ and linewidth function $\Gamma_L(\epsilon)$ are left unspecified. In the numerical example of Sec. III, the equilibrium Green's function $\tilde{G}^r(\omega)$ is known exactly in closed form^{23,31} for the linewidth function $\Gamma_L(\epsilon)$ in Eq. (19), hence Eq. (A5) can be calculated explicitly.

After the t_1 integral, the second term in Eq. (A4) reads

$$\int \frac{d\omega d\omega_1}{2\pi 2\pi i} \int_{-\infty}^{E_F} \frac{d\epsilon}{2\pi} \frac{i\tilde{G}^r(\omega)\bar{G}^r(\omega_1)\Gamma_L(\epsilon)}{i(\omega_1-\epsilon-\Delta-i0^+)} e^{-i(\omega-\epsilon)t} \\ \times \left(\frac{\Delta_c}{\omega-\omega_1-i0^+} + \frac{\Delta(\tilde{\Sigma}_L^r(\omega_1-\Delta)-\tilde{\Sigma}_L^r(\omega))}{(\omega_1-\omega-\Delta+i0^+)(\omega_1-\omega+i0^+)} \right).$$

The ω_1 integration can be carried out by contour integration in the upper half-plane where there are no unknown poles in ω_1 . By the residue theorem, the last expression becomes

$$\int \frac{d\omega}{2\pi} \int_{-\infty}^{E_F} \frac{d\epsilon}{2\pi} \tilde{G}^r(\omega)\bar{G}^r(\epsilon+\Delta)\Gamma_L(\epsilon) e^{-i(\omega-\epsilon)t} \\ \times \left[\frac{\Delta_c}{\omega-\epsilon-\Delta-i0^+} + \frac{\Delta(\tilde{\Sigma}_L^r(\epsilon)-\tilde{\Sigma}_L^r(\omega))}{(\epsilon-\omega+i0^+)(\epsilon+\Delta-\omega+i0^+)} \right]. \quad (\text{A6})$$

Again, this expression cannot be simplified further without

the knowledge of the equilibrium Green's function \tilde{G}^r and the linewidth function Γ_L . This completes the calculation of the first term of Eq. (A2).

We now calculate the second term of Eq. (A2). In this case, integration over t_1 generates $-1/(\omega-\epsilon+i0^+)$ and the second term of Eq. (A2) becomes

$$\int \frac{d\omega}{2\pi} \int_{-\infty}^{E_F} \frac{d\epsilon}{2\pi} e^{-i(\omega-\epsilon)t} \frac{-\tilde{G}^r(\omega)\Gamma_L(\epsilon)}{(\omega-\epsilon+i0^+)}. \quad (\text{A7})$$

Using the Plemelj formula $1/(\omega \pm i0^+) = P(1/\omega) \mp i\pi\delta(\omega)$, this last expression becomes

$$\int \frac{d\omega}{2\pi} \int_{-\infty}^{E_F} \frac{d\epsilon}{2\pi} i\tilde{G}^r(\omega)\Gamma_L(\epsilon) \frac{e^{-i(\omega-\epsilon)t}}{\omega-\epsilon-i0^+} + \int_{-\infty}^0 \frac{d\epsilon}{2\pi} i\tilde{G}^r(\epsilon)\Gamma_L(\epsilon), \quad (\text{A8})$$

so that all the poles in the lower ω half-plane are those of the equilibrium Green's function. No further simplifications can be made in Eq. (A8) unless \tilde{G}^r and Γ_L are known. This completes the calculation of the second term in Eq. (A2). Summing up Eqs. (A5), (A6), and (A8), we obtain the final result for Eq. (A2),

$$\int dt_1 \tilde{G}^r(t, t_1) \tilde{\Sigma}_L^<(t_1, t) = \int_{-\infty}^{E_F} \frac{d\epsilon}{2\pi} \left[i\tilde{G}^r(\epsilon)\Gamma_L(\epsilon) + \int \frac{d\omega}{2\pi} \frac{\Delta\tilde{G}^r(\omega)\Gamma_L(\epsilon)e^{-i(\omega-\epsilon)t}}{(\omega-\epsilon-\Delta-i0^+)(\omega-\epsilon-i0^+)} \right. \\ \left. + \int \frac{d\omega}{2\pi} \tilde{G}^r(\omega)\bar{G}^r(\epsilon+\Delta)\Gamma_L(\epsilon) e^{-i(\omega-\epsilon)t} \left(\frac{\Delta_c}{\omega-\epsilon-\Delta-i0^+} + \frac{\Delta(\tilde{\Sigma}_L^r(\epsilon)-\tilde{\Sigma}_L^r(\omega))}{(\omega-\epsilon-i0^+)(\omega-\epsilon-\Delta-i0^+)} \right) \right]. \quad (\text{A9})$$

By a similar procedure, the second term of expression (A1) is found to be

$$\int dt_1 \tilde{G}^<(t, t_1) \tilde{\Sigma}_L^a(t_1, t) = \int_{-\infty}^{E_F} \frac{d\epsilon}{2\pi} \left\{ i \sum_{\alpha} A_{\alpha}(\epsilon, t) \Gamma_{\alpha}(\epsilon) \tilde{G}^a(\epsilon) \tilde{\Sigma}_L^a(\epsilon) + \int \frac{d\omega}{2\pi} \sum_{\alpha} \frac{e^{i(\omega-\epsilon)t}}{\omega-\epsilon+i0^+} A_{\alpha}(\epsilon, t) \Gamma_{\alpha}(\epsilon) \tilde{G}^a(\epsilon) \tilde{\Sigma}_L^a(\omega) \right. \\ \left. + \int \frac{d\omega}{2\pi} \sum_{\alpha} \frac{e^{i(\omega-\epsilon)t} A_{\alpha}(\epsilon, t) \Gamma_{\alpha}(\epsilon) \bar{G}^a(\epsilon+\Delta_{\alpha}) \tilde{\Sigma}_L^a(\omega)}{\epsilon+\Delta_{\alpha}-\omega-\Delta-i0^+} + \sum_{\alpha} i A_{\alpha}(\epsilon, t) \Gamma_{\alpha}(\epsilon) \int \frac{d\omega d\omega_1}{2\pi i 2\pi i} \frac{e^{i(\omega_1-\epsilon)t}}{\omega-\omega_1+i0^+} \tilde{G}^a(\omega) \right. \\ \left. \times \left[\frac{\Delta_{\alpha}}{\omega-\epsilon+i0^+} + \left(\Delta_c - \sum_{\beta} \frac{\Delta_{\beta}(\tilde{\Sigma}_{\beta}^a(\omega)-\tilde{\Sigma}_{\beta}^a(\epsilon+\Delta_{\alpha}-\Delta_{\beta}))}{\omega-\epsilon-\Delta_{\alpha}+\Delta_{\beta} \pm i0^+} \right) \bar{G}^a(\epsilon+\Delta_{\alpha}) \right] \tilde{\Sigma}_L^a(\omega_1) \right\}. \quad (\text{A10})$$

Finally, summing up expressions (A9) and (A10), we obtain the final result for expression (A1). In practical calculations, we first evaluate the equilibrium (tilded) and steady-state (barred) quantities of the two-probe device. These quantities are then inserted into Eqs. (A9) and (A10), so that together with Eq. (15), the first term of Eq. (17) can be obtained.

For the sake of completeness, in the following, we give explicit expressions for the remaining terms in Eq. (17). These are derived following the procedure presented above. We have

$$\begin{aligned}
& \int dt_1 G^r(t, t_1) \tilde{\Sigma}_L^a(t_1, t) \\
&= \left[\int \frac{d\omega}{2\pi i} \frac{d\omega_1}{2\pi} \frac{\Delta e^{i(\omega-\omega_1)t} \tilde{G}^r(\omega_1) \tilde{\Sigma}_L^a(\omega)}{(\omega_1 - \omega - \Delta - i0^+)(\omega_1 - \omega - i0^+)} \right. \\
&+ \int \frac{d\omega}{2\pi} \tilde{G}^r(\omega) \tilde{\Sigma}_L^a(\omega) + \int \frac{d\omega d\omega_2}{2\pi 2\pi i} e^{i(\omega_2-\omega)t} \tilde{G}^r(\omega) \bar{G}^r(\omega_2 + \Delta) \tilde{\Sigma}_L^a(\omega_2) \left[\frac{\Delta_c}{\omega - \omega_2 - \Delta - i0^+} \right. \\
&\left. \left. + \frac{\Delta(\tilde{\Sigma}_L^r(\omega_2) - \tilde{\Sigma}_L^r(\omega_2))}{(\omega_2 - \omega + i0^+)(\omega_2 + \Delta - \omega + i0^+)} \right] \right], \tag{A11}
\end{aligned}$$

$$\begin{aligned}
& \int dt_1 dt_2 \Sigma_L^r(t, t_1) G^r(t_1, t_2) \Sigma_L^a(t_2, t) \\
&= \int \frac{d\omega_1}{2\pi i} \frac{d\omega_2}{2\pi i} e^{i(\omega_2-\omega_1)t} \tilde{\Sigma}_L^r(\omega_1) \left(\frac{\bar{G}^r(\omega_2 + \Delta)}{\omega_1 - \omega_2 - i0^+} - \frac{\tilde{G}^r(\omega_1)}{\omega_1 - \omega_2 + i0^+} \right) \tilde{\Sigma}_L^a(\omega_2) \\
&+ \int \frac{d\omega_1}{2\pi i} \frac{d\omega_2}{2\pi i} \frac{d\omega}{2\pi} \frac{\tilde{\Sigma}_L^r(\omega_1) \tilde{G}^r(\omega) \tilde{\Sigma}_L^a(\omega_2)}{(\omega - \omega_1 - i0^+)(\omega - \omega_2 - \Delta - i0^+)} e^{i(\omega_2-\omega_1)t} \\
&+ \int \frac{d\omega_1}{2\pi i} \frac{d\omega_2}{2\pi i} \frac{d\omega}{2\pi} e^{i(\omega_2-\omega_1)t} \frac{\tilde{\Sigma}_L^r(\omega_1) \tilde{\Sigma}_L^a(\omega_2) \tilde{G}^r(\omega) \bar{G}^r(\omega_2 + \Delta)}{\omega - \omega_1 - i0^+} \left[\frac{\Delta_c}{\omega - \omega_2 - \Delta - i0^+} + \frac{\Delta(\tilde{\Sigma}_L^r(\omega_2) - \tilde{\Sigma}_L^r(\omega))}{(\omega_2 - \omega + i0^+)(\omega_2 + \Delta - \omega + i0^+)} \right], \tag{A12}
\end{aligned}$$

$$\begin{aligned}
& \int dt_1 dt_2 \Sigma_L^r(t, t_1) G^r(t_1, t_2) \Sigma_L^<(t_2, t) \\
&= \int_{-\infty}^{E_F} \frac{d\epsilon}{2\pi} \left[\int \frac{d\omega_1}{2\pi i} e^{i(\omega_2-\omega_1)t} \tilde{\Sigma}_L^r(\omega_1) \left(\frac{\bar{G}^r(\omega_2 + \Delta)}{\omega_1 - \epsilon - i0^+} - \frac{\tilde{G}^r(\omega_1)}{\omega_1 - \omega_2 + i0^+} \right) \bar{\Gamma}_L(\epsilon) \right. \\
&+ \int \frac{d\omega_1}{2\pi i} \frac{d\omega}{2\pi} \frac{\tilde{\Sigma}_L^r(\omega_1) \tilde{G}^r(\omega) \bar{\Gamma}_L(\epsilon)}{(\omega - \omega_1 - i0^+)(\omega - \epsilon - \Delta - i0^+)} e^{i(\epsilon-\omega_1)t} + \int \frac{d\omega_1}{2\pi i} \frac{d\omega}{2\pi} e^{i(\epsilon-\omega_1)t} \frac{\tilde{\Sigma}_L^r(\omega_1) \bar{\Gamma}_L(\epsilon) \tilde{G}^r(\omega) \bar{G}^r(\epsilon + \Delta)}{\omega - \omega_1 - i0^+} \left(\frac{\Delta_c}{\omega - \epsilon - \Delta - i0^+} \right. \\
&\left. \left. + \frac{\Delta(\tilde{\Sigma}_L^r(\epsilon) - \tilde{\Sigma}_L^r(\omega))}{(\epsilon - \omega + i0^+)(\epsilon + \Delta - \omega + i0^+)} \right) \right], \tag{A13}
\end{aligned}$$

$$\begin{aligned}
& \int dt_1 dt_2 \Sigma_L^r(t, t_1) G^<(t_1, t_2) \Sigma_L^a(t_2, t) \\
&= \int_{-\infty}^{E_F} \frac{d\epsilon}{2\pi} \left\{ \int \frac{d\omega_1}{2\pi i} \frac{d\omega_2}{2\pi i} e^{i(\omega_2-\omega_1)t} \sum_{\alpha} \frac{\tilde{\Sigma}_L^r(\omega_1) \bar{G}^r(\epsilon + \Delta_{\alpha}) \Gamma_{\alpha}(\epsilon) \bar{G}^a(\epsilon + \Delta_{\alpha}) \tilde{\Sigma}_L^a(\omega_2)}{(\omega_1 + \Delta - \epsilon - \Delta_{\alpha} - i0^+)(\epsilon + \Delta_{\alpha} - \omega_2 - \Delta - i0^+)} + 2i \operatorname{Im} \left\{ \int \frac{d\omega_1}{2\pi i} \frac{d\omega_2}{2\pi i} \right. \right. \\
&- i e^{i(\omega_2-\omega_1)t} \sum_{\alpha} \frac{\tilde{\Sigma}_L^r(\omega_1) \tilde{G}^r(\epsilon) \Gamma_{\alpha}(\epsilon) \bar{G}^a(\epsilon + \Delta_{\alpha}) \tilde{\Sigma}_L^a(\omega_2)}{(\omega_1 - \epsilon - i0^+)(\epsilon + \Delta_{\alpha} - \omega_2 - \Delta - i0^+)} + \int \frac{d\omega_2}{2\pi i} i \sum_{\alpha} \frac{\tilde{\Sigma}_L^r(\epsilon) \tilde{G}^r(\epsilon) \Gamma_{\alpha}(\epsilon) \bar{G}^a(\epsilon + \Delta_{\alpha}) \tilde{\Sigma}_L^a(\omega_2)}{\epsilon + \Delta_{\alpha} - \omega_2 - \Delta - i0^+} e^{i(\omega_2-\epsilon)t} \\
&- \int \frac{d\omega_1}{2\pi i} \frac{d\omega_2}{2\pi i} \frac{d\omega}{2\pi i} i \sum_{\alpha} \frac{\tilde{\Sigma}_L^r(\omega_1) \tilde{G}^r(\omega)}{\omega - \epsilon - \Delta_{\alpha} - i0^+} \left[\frac{\Delta_{\alpha}}{\omega - \epsilon - i0^+} + \left(\Delta_c - \sum_{\beta} \frac{\Delta_{\beta}(\tilde{\Sigma}_L^r(\omega) - \tilde{\Sigma}_L^r(\epsilon + \Delta_{\alpha} - \Delta_{\beta}))}{\omega - \epsilon - \Delta_{\alpha} + \Delta_{\beta} \pm i0^+} \right) \bar{G}^r(\epsilon + \Delta_{\alpha}) \right] \\
&\times \frac{\Gamma_{\alpha}(\epsilon) \bar{G}^a(\epsilon + \Delta_{\alpha})}{\omega_1 - \omega + i0^+} \frac{\tilde{\Sigma}_L^a(\omega_2) e^{i(\omega_2-\omega_1)t}}{\epsilon + \Delta_{\alpha} - \omega_2 - \Delta - i0^+} \left. \right\} + \int \frac{d\omega_1}{2\pi i} \frac{d\omega_2}{2\pi i} i \sum_{\alpha} e^{i(\omega_2-\omega_1)t} \frac{\tilde{\Sigma}_L^r(\omega_1) \tilde{G}^r(\epsilon) \Gamma_{\alpha}(\epsilon) \bar{G}^a(\epsilon) \tilde{\Sigma}_L^a(\omega_2)}{(\omega_1 - \epsilon + i0^+)(\epsilon - \omega_2 + i0^+)} \\
&+ \int \frac{d\omega_1}{2\pi i} \frac{d\omega_2}{2\pi i} \frac{d\omega}{2\pi i} i \sum_{\alpha} e^{i(\omega_2-\omega_1)t} \frac{\tilde{\Sigma}_L^r(\omega_1) \tilde{G}^r(\omega) F_{\alpha}(\omega, \epsilon) \Gamma_{\alpha}(\epsilon) \bar{G}^a(\epsilon) \tilde{\Sigma}_L^a(\omega_2)}{(\omega - \epsilon - \Delta_{\alpha} - i0^+)(\omega_1 - \omega + i0^+)(\epsilon - \omega_2 + i0^+)}
\end{aligned}$$

$$\begin{aligned}
& - \int \frac{d\omega_1 d\omega_2 d\Omega}{2\pi i 2\pi i 2\pi i} i \sum_{\alpha} e^{i(\omega_2 - \omega_1)t} \frac{\tilde{\Sigma}_L^r(\omega_1) \tilde{G}^r(\epsilon) \Gamma_{\alpha}(\epsilon) \tilde{G}^a(\Omega) F_{\alpha}^{\dagger}(\Omega, \epsilon) \tilde{\Sigma}_L^a(\omega_2)}{(\omega_1 - \epsilon + i0^+)(\Omega - \epsilon - \Delta_{\alpha} + i0^+)(\Omega - \omega_2 + i0^+)} \\
& - \int \frac{d\omega_1 d\omega_2 d\Omega}{2\pi i 2\pi i 2\pi i} i \sum_{\alpha} \frac{\tilde{\Sigma}_L^r(\omega_1) \tilde{G}^r(\omega) F_{\alpha}(\omega, \epsilon) e^{i(\omega_2 - \omega_1)t}}{(\omega_1 - \omega + i0^+)(\omega - \epsilon - \Delta_{\alpha} - i0^+)} \Gamma_{\alpha}(\epsilon) \frac{\tilde{\Sigma}_L^a(\omega_2) \tilde{G}^a(\Omega) F_{\alpha}^{\dagger}(\Omega, \epsilon)}{(\Omega - \omega_2 + i0^+)(\Omega - \epsilon - \Delta_{\alpha} + i0^+)} \Bigg\}, \quad (\text{A14})
\end{aligned}$$

where we have defined

$$F_{\alpha}(\omega, \epsilon) \equiv \frac{\Delta_{\alpha}}{\omega - \epsilon - i0^+} + \left(\Delta_c - \sum_{\beta} \Delta_{\beta} \frac{\tilde{\Sigma}_{\beta}^r(\omega) - \tilde{\Sigma}_{\beta}^r(\epsilon + \Delta_{\alpha} - \Delta_{\beta})}{\omega - \epsilon - \Delta_{\alpha} + \Delta_{\beta} \pm i0^+} \right) \tilde{G}^r(\epsilon + \Delta_{\alpha}).$$

Although expressions (A9)–(A14) appear to be very complicated, the right-hand side of these expressions involves only steady-state (barred) or equilibrium (tilded) quantities. Therefore, for any given two-probe device, these quantities can be calculated first from a conventional dc transport analysis and then inserted into expressions (A9)–(A14) for the analysis of transient current-current correlations given by Eq. (17). Equilibrium and steady-state Green's functions and self-energies can be calculated from well-developed first principles methods^{36,37} that include all atomistic degrees of freedom. The theory presented in this work can be therefore used, in principle, to analyze transient current-current correlations in realistic device structures including microscopic details of the system.

*Present address: Department of Physics, Stanford University, Stanford, CA 94305-4045, USA.

¹Ya. M. Blanter and M. Büttiker, Phys. Rep. **336**, 1 (2000).

²W. Schottky, Ann. Phys. **57**, 541 (1918).

³R. Landauer, Nature (London) **392**, 658 (1998).

⁴T. Gramspacher and M. Büttiker, Phys. Rev. Lett. **81**, 2763 (1998).

⁵L. Saminadayar, D. C. Glattli, Y. Jin, and B. Etienne, Phys. Rev. Lett. **79**, 2526 (1997).

⁶F. Lefloch, C. Hoffmann, M. Sanquer, and D. Quirion, Phys. Rev. Lett. **90**, 067002 (2003).

⁷M. Büttiker, Phys. Rev. B **46**, 12485 (1992).

⁸M. Henny, S. Oberholzer, C. Strunk, T. Heinzel, K. Ensslin, M. Holland, and C. Schönberger, Science **284**, 296 (1999).

⁹J. R. Pierce, Bell Syst. Tech. J. **27**, 158 (1948).

¹⁰V. A. Khlus, Zh. Eksp. Teor. Fiz. **93**, 2179 (1987) [Sov. Phys. JETP **66**, 1243 (1987)].

¹¹M. Büttiker, Phys. Rev. Lett. **65**, 2901 (1990).

¹²E. Onac, F. Balestro, L. H. Willems van Beveren, U. Hartmann, Y. V. Nazarov, and L. P. Kouwenhoven, Phys. Rev. Lett. **96**, 176601 (2006).

¹³L. P. Kouwenhoven, S. Jauhar, J. Orenstein, P. L. McEuen, Y. Nagamune, J. Motohisa, and H. Sakaki, Phys. Rev. Lett. **73**, 3443 (1994).

¹⁴L. P. Kouwenhoven, A. T. Johnson, N. C. van der Vaart, C. J. P. M. Harmans, and C. T. Foxon, Phys. Rev. Lett. **67**, 1626 (1991).

¹⁵W. Lu, Z. Ji, L. Pfeiffer, K. W. West, and A. J. Rimberg, Nature (London) **423**, 422 (2003).

¹⁶M. Büttiker, J. Phys.: Condens. Matter **5**, 9361 (1993); M. Büttiker, H. Thomas, and A. Prêtre, Phys. Lett. A **180**, 364 (1993).

¹⁷J. Gabelli, G. Fève, J.-M. Berroir, B. Plaçais, A. Cavanna, B. Etienne, Y. Jin, and D. C. Glattli, Science **313**, 499 (2006).

¹⁸J. Wang, B. Wang, and H. Guo, Phys. Rev. B **75**, 155336 (2007).

¹⁹M. Switkes, C. Marcus, K. Capman, and A. C. Gossard, Science **283**, 1905 (1999).

²⁰B. Wang, J. Wang, and H. Guo, Phys. Rev. B **65**, 073306 (2002).

²¹R. J. Schoelkopf, P. Wahlgren, A. A. Kozhevnikov, P. Delsing,

and D. E. Prober, Science **280**, 1238 (1998).

²²J. Maciejko, J. Wang, and H. Guo, Phys. Rev. B **74**, 085324 (2006).

²³T. Kwapinski, R. Taranko, and E. Taranko, Phys. Rev. B **66**, 035315 (2002).

²⁴N. S. Wingreen, A. P. Jauho, and Y. Meir, Phys. Rev. B **48**, 8487 (1993).

²⁵A. P. Jauho, N. S. Wingreen, and Y. Meir, Phys. Rev. B **50**, 5528 (1994).

²⁶H. Haug and A. P. Jauho, *Quantum Kinetics in Transport and Optics of Semiconductors* (Springer, Berlin, 1998).

²⁷G. D. Mahan, *Many-Particle Physics* (Academic, New York, 2000).

²⁸D. C. Langreth, in *Linear and Nonlinear Electron Transport in Solids* edited by J. T. Devreese and V. E. van Doren, NATO Advanced Studies Institute, Series B: Physics (Plenum, New York, 1976), Vol. 17.

²⁹N. S. Wingreen and Y. Meir, Phys. Rev. B **49**, 11040 (1994).

³⁰T. Fujisawa, T. Oosterkamp, W. G. van der Wiel, B. W. Broer, R. Aguado, S. Tarucha, and L. P. Kouwenhoven, Science **282**, 932 (1998).

³¹Y. Zhu, J. Maciejko, T. Ji, H. Guo, and J. Wang, Phys. Rev. B **71**, 075317 (2005).

³²Y. Wei, B. Wang, J. Wang, and H. Guo, Phys. Rev. B **60**, 16900 (1999).

³³W. C. van Etten, *Introduction to Random Signals and Noise* (Wiley, New York, 2005).

³⁴U. Fano, Phys. Rev. **72**, 26 (1947).

³⁵The steady-state Fano factor μ at zero temperature can be obtained (Ref. 32) as $\mu = \frac{1}{2e\langle I \rangle} \int dE (F_L(E) - F_R(E))^2 (1 - T) T$, where F_L and F_R are the Fermi functions of the left and right leads, respectively, and T is the transmission coefficient. At equilibrium and for resonant transmission $T = 1$, the Fano factor reduces to zero.

³⁶J. Taylor, H. Guo, and J. Wang, Phys. Rev. B **63**, 245407 (2001).

³⁷D. Waldron, V. Timoshevskii, Y. Hu, K. Xia, and H. Guo, Phys. Rev. Lett. **97**, 226802 (2006).